Enhancement of Mixing in Reacting Fuel-Rich Plumes Issued from Elliptical Nozzles

K.C. Schadow,* K.J. Wilson,† and M.J. Lee‡
Naval Weapons Center, China Lake, California
and
E. Gutmark§
University of Southern California, Los Angeles, California

The mixing of jets and reacting fuel-rich plumes issued from elliptical and circular nozzles was compared in the tests reported in this paper. In nonreacting tests with hotwire probes, the jet issued from an elliptical nozzle mixed faster with a coaxial, ducted airstream than a jet issued from a circular nozzle. In combustion tests with thermocouples, mixing between the reacting fuel-rich plume and the coaxial air was also enhanced with elliptical nozzles. This resulted in higher local combustion temperatures and therefore higher reaction rates near the nozzle exit. In both cases, the tests were done at high Reynolds numbers and turbulent initial conditions.

Nomenclature

$A_{t,\mathrm{CIRC}}$ = throat area of circular nozzle
$A_{t,2:1}$ = throat area of elliptical nozzle (2:1 aspect ratio)
D = duct diameter
D_C = combustor diameter
D_{CIRC} = circular nozzle diameter
D_{MAJ} = major axis length
D_{MIN} = minor axis length
E_v = energy of velocity fluctuations
f = frequency
f_i = initial vortex shedding frequency
$\dot{m}_A$ = air mass flow rate
$\dot{m}_{\mathrm{CH}}$ = ethylene mass flow rate
$\dot{m}_{\mathrm{N}}$ = nitrogen mass flow rate
$\dot{m}_{\mathrm{O}}$ = oxygen mass flow rate
P_A = air feed system pressure
P_C = combustor pressure
R = radial direction
R_C = radius of combustion chamber
Re = Reynolds number
$R_{0.5}$ = jet half-width
St = Strouhal number
St_i = Strouhal number based on f_i
T = temperature
T_C = combustor temperature
U = velocity
U_0 = jet exit velocity
X = axial direction
θ_0 = momentum thickness at nozzle exit
Φ = equivalence ratio

Introduction

FUEL-RICH plume combustion in a ducted, subsonic airstream involves several interrelated physical and chemical processes.[1,2] Two critical features for achieving high-energy release are 1) the turbulent mixing process between fuel-rich products and air and 2) the initiation of combustion in the local mixing region with near-stoichiometric mixture ratios or with highest possible combustion temperatures. Both features are discussed in the following for the coaxial plume/air mixing process.

The turbulent mixing process between the nonreacting plume (jet) and the air occurs in a mixing layer that is governed by vortex shedding and subsequent vortex interactions. Vortex shedding at the nozzle exit occurs as a result of mixing layer instability waves that grow and subsequently roll up into vortices. The roll-up occurs at the most amplified frequency f_i. This frequency, when scaled with the initial shear layer momentum thickness θ_0 and the jet exit velocity U_0 yields a Strouhal number $St_i = f_i \cdot \theta_0 / U_0$, which is predicted to be $St_i = 0.017$ by the linear instability theory.[3]

The shear layer dynamics discussed here were investigated experimentally in many laboratory jet and shear layer facilities. Recently, they were also measured in a high Reynolds number jet with highly turbulent initial conditions.[4] These tests were conducted in both a free circular jet and a ducted jet with and without acoustic forcing.

The generation of vortices and their subsequent growth are associated with outside fluid entrainment into the jet flow. Through this process, the jet fluid is mixed with the surrounding fluid. Various methods of mixing enhancement by active shear layer control have been suggested. These methods introduce external forcing into the shear layer. The artificially generated perturbations change the downstream development of the mixing layer.

A passive method for increasing the jet entrainment, and consequently its mixing, was proposed by Gutmark and Ho.[5,6] They showed that an unforced jet injected from a small-aspect-ratio elliptical nozzle entrained up to eight times more fluid than a circular jet. This feature was attributed to complex dynamics and the self-induction of elliptic vortices formed as a result of the initial instability of the jet. The elliptical vortices switched their major and minor axes as they were convected downstream. This motion was accompanied by the deformation of the vortex cross section and the development of azimuthal instabilities. As a result of these processes, small-scale fluctuations were formed and small-scale mixing was augmented in the initial region of the jet.[7]

Received Nov. 20, 1985; revision received July 30, 1986.

*Supervisory General Engineer.
†Aerospace Engineer.
‡Mechanical Engineer.
§Visiting Professor, presently with the Naval Weapons Center.

Past work with elliptical jets was performed at low Reynolds numbers, laminar initial conditions, and nonreacting free-jet conditions. In the present work, the effect of elliptical jets on turbulent mixing was studied at high Reynolds numbers, with turbulent initial conditions, with and without combustion, and with a coaxial airflow.

For achieving high heat release, it is also important to initiate autoignition of the fuel-rich products in the local mixing regions with near-stoichiometric mixture ratios. This is necessary to achieve the highest possible (near stoichiometric) local combustion temperatures and, therefore, the highest possible reaction rates. This is critical for fuel-rich plumes containing particulate fuels.[8]

In a coaxial mixing region with overall above-stoichiometric air-to-fuel ratios, or equivalence ratios of less than one ($\Phi<1$), near-stoichiometric mixture ratios exist in the extreme fore end of the mixing region, as generally predicted by turbulent models and also shown in experiments.[9] Therefore, for achieving highest possible local combustor temperatures, it is necessary to initiate combustion of the fuel-rich products in the extreme fore end of the coaxial mixing region. However, experiments showed that combustion did not occur near the plume exit and a lifted diffusion flame resulted.[10] When ignition occurred several nozzle diameters downstream of the nozzle exit, the combustion temperatures were significantly below the near-stoichiometric temperatures.[9,11] This was a result of excessive mixing of air with the fuel-rich plume before combustion was initiated. Combustion probably did not occur in the extreme fore end of the mixing region near the nozzle because of limited mixing on the molecular scale in the presence of large-scale vortices. This was especially the case when the plume exhaust velocity was supersonic and the duct pressure was low. The combustion temperatures were higher when the exhaust velocity was reduced to subsonic speed and combustion occurred at the beginning of the mixing region.[12]

The previous results were obtained when circular nozzles were used. In the present study, elliptical nozzles were used in an attempt to enhance overall mixing between the fuel-rich plume and the airstream and to enhance combustion in the extreme fore end of the coaxial mixing region with highest possible combustion temperatures.

Specifically, the objectives of the present study were 1) to compare the mixing rates of elliptical nozzles with those of circular nozzles and to determine the initial shear layer instability frequencies for both nozzles in nonreacting and coaxial flow experiments using a hot-wire anemometer; and 2) to measure combustion temperatures in the fore end of the mixing region using thermocouples for gaseous fuel-rich plumes issued from circular and elliptical nozzles.

Experimental Setup

A chamber with an inner diameter of $D_C=5.3$ in. (13.5 cm) was used for both the nonreacting and combustion tests.

In the nonreacting tests (Fig. 1), the fuel-rich exhaust was replaced by air which was introduced into the mixing section through a 0.75 in. (1.9 cm) diameter pipe. Interchangeable nozzles with circular and near-elliptical cross sections were located at the downstream end of the pipe, as will be described in detail later. The air was introduced into the mixing section through a grid and a honeycomb. The total air mass flow of $\dot{m}_A=0.67$ lb/s (0.30 kg/s) was divided into two parts in a ratio of 13.2:1 (air to "fuel") by proper selection of sonic orifices in the air feeding system. Based on this air mass flow ratio and the geometric pipe diameter, the initial velocities of the air and the fuel were calculated to be $U=40$ and 130 ft/s (12.2 and 40 m/s), respectively. The velocity of the fuel flow corresponds to a Reynolds number of $Re=8\times10^4$ based on $D=0.75$ in. (1.9 cm), ambient air temperature, and a chamber pressure of $P_{C,AIR}=20.8$ psia (143 kPa). The velocity field in the mixing section was measured using a constant-temperature, hot-wire anemometer. To determine the shear layer instability frequencies related to the vortex dynamics, the hot-wire signals were digitized and analyzed using a PDP 11/55 minicomputer.

For the reacting flow tests, a precombustor that burns ethylene (CH), oxygen (O), and nitrogen (N) was used. The experimental setup had the same geometrical dimensions as the one used for the cold-flow tests. The gaseous fuels were ignited in the precombustor by a hydrogen/oxygen pilot igniter. Mass flow rates of the precombustor were $\dot{m}_{CH}=0.075$ lb/s (0.034 kg/s), $\dot{m}_0=0.076$ lb/s (0.034 kg/s), and $\dot{m}_N=0.089$ lb/s (0.040 kg/s). The air mass flow was 2 lb/s (0.9 kg/s). The initial temperature and velocity of the air were $T=280$ K and $U=30$ ft/s (9 m/s) for a chamber pressure of $P_C=80$ psia (552 kPa). The initial conditions of the fuel-rich reaction products were $T=1650$ K and $U=1500$ ft/s (450 m/s).[11]

In a limited number of tests, direct color photographs of the combustion zone near the plume nozzle were taken through a plexiglas-walled combustor section.

One circular and three elliptical nozzles were used for the nonreacting and combustion tests. The circular nozzle had a diameter of $D_{CIRC}=0.75$ in. (1.9 cm), which was equal to the pipe diameter D, and the three elliptical nozzles had major-to-minor axis ratios of $D_{MAJ}/D_{MIN}=2{:}1$, 3:1, and 3.5:1. The area of each of the four nozzle cross sections was nearly the same. Most of the measurements reported were done with the 3:1 ratio nozzle for reasons that will be explained later. The elliptical nozzles were made by pressing circular pipes. The resulting cross sections did not have an exact elliptical shape, but to simplify the writing they will be called "elliptical" hereafter. The transition from the circular to the elliptical cross section occurred over an axial pipe length of 6 in. (12.2 cm).

Test Results

Nonreacting Tests

The initial mean velocity profiles of the circular jet and the 3:1 elliptical jet, measured at different axial cross sections from the jet nozzle plane ($X/D_{CIRC}=0.17$–13.3) are shown in Figs. 2–4.

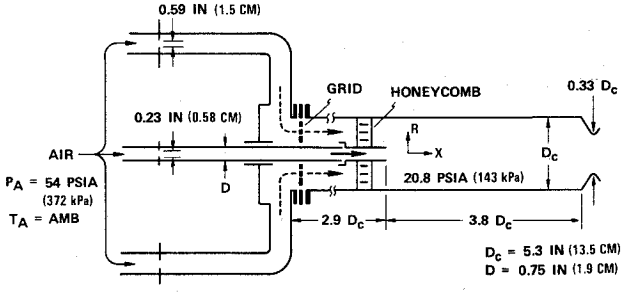

Fig. 1 Test setup for nonreacting tests.

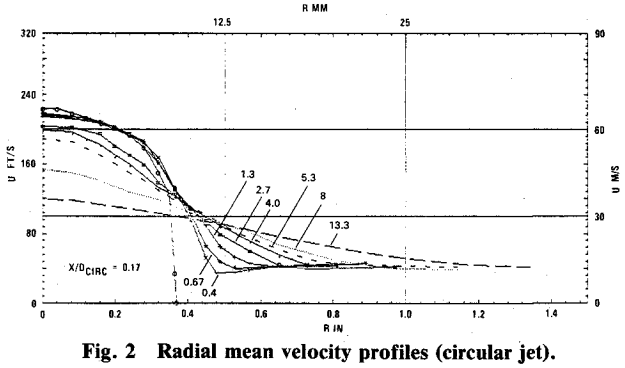

Fig. 2 Radial mean velocity profiles (circular jet).

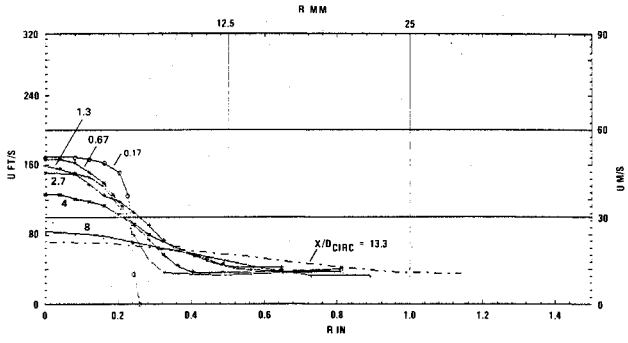

Fig. 3 Radial mean velocity profiles (elliptical jet, 3:1, minor axis).

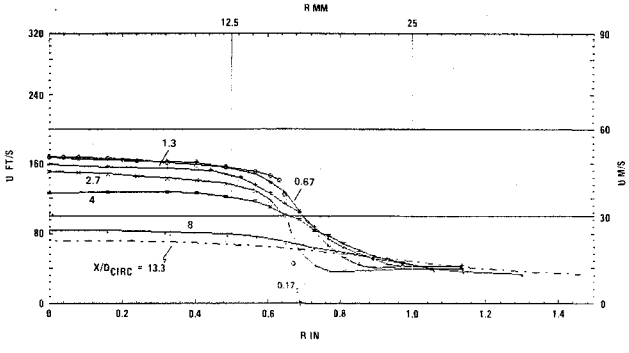

Fig. 4 Radial mean velocity profiles (elliptical jet, 3:1, major axis).

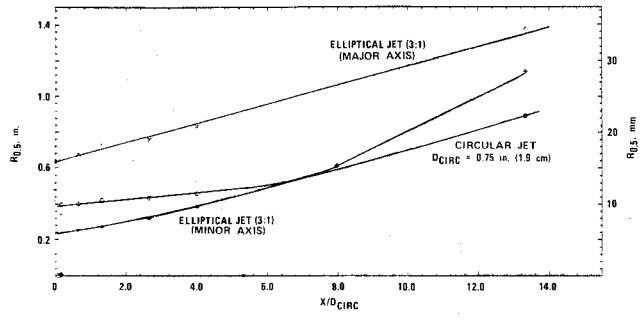

Fig. 5 Spreading rates for circular and elliptical (3:1) jets.

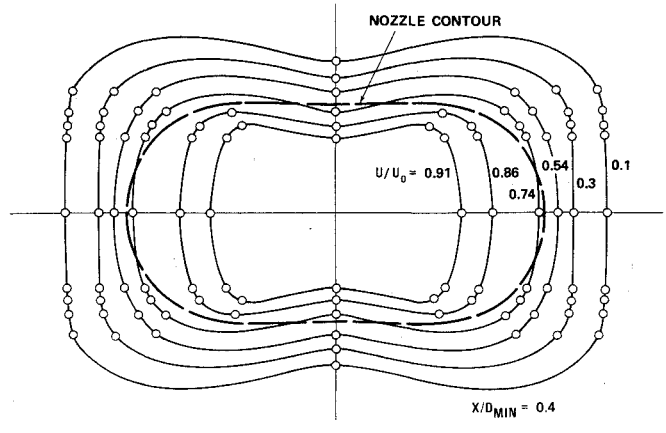

Fig. 6 Constant velocity contours (elliptical jet, 2:1).

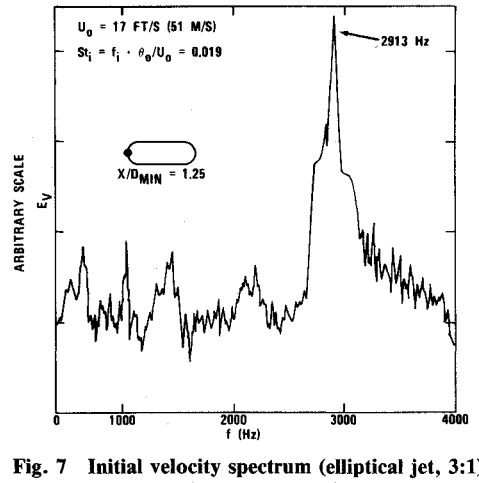

Fig. 7 Initial velocity spectrum (elliptical jet, 3:1).

The initial mean velocity profiles ($X/D_{CIRC}=0.17$), which resemble fully developed turbulent pipe flows, were quite different from those of regular laboratory-type jets with "top-hat" exit velocity profiles. From the initial mean velocity profiles $X/D=0.17$, the initial mixing layer momentum thicknesses were determined for the circular jet [$\theta_0=0.0334$ in. (0.85 mm)] and the elliptical jet [$\theta_0=0.0117$ in. (0.3 mm) on the minor axis plane and $\theta_0=0.0132$ in. (0.34 mm) on the major axis plane]. These measurements show that θ_0 varied almost 13% around the circumference of the elliptical nozzle exit. This is different from a circular jet, which has a uniform θ_0 distribution around its circumference. This initial shear layer momentum thickness can be used, according to the linear instability theory,[3] to calculate the shedding frequency at the jet exit.

From the mean velocity profiles, it may be seen that the circular jet grew slowly into the coaxial airstream, especially for $X/D_{CIRC}<5.3$ (Fig. 2), while the elliptical jet exhibited a strong spreading into the surrounding airstream in both the minor and major axis planes (Figs. 3 and 4).

The spreading rates of the circular and elliptical jets are shown in Fig. 5 where the widths of the two jets are compared. The jet width is defined here as the distance from the jet axis to where the mean velocity drops to 50% of its maximum value ($R_{0.5}$). It may be seen that the elliptical jet spreads faster on the minor and major planes than the circular jet. The jet width on the minor axis equaled the circular jet diameter at $X/D_{CIRC}=6$, but was still smaller than the major axis even at $X/D_{CIRC}=13.3$. No switching between the minor and major axes of the jet was observed in the range of the present measurements. The larger spreading rate of the jet in the minor axis plane relative to the major axis plane shows that both sides become equal at about 18 equivalent diameters from the exit.

The mean velocity measurements also showed that the flow of the 2:1 elliptical jet near the nozzle ($X/D_{MIN}=0.4$) was more complicated than expected in regular jets. The velocity contours in Fig. 6 show that the flow did not fully match the shape of the nozzle and some kinks developed on the major axis side, indicating the development of higher azimuthal modes.

The velocity fluctuation spectra in the shear layer around the jet exit circumference, as determined by power spectral density analysis, were measured in the circular and elliptical jets. The spectrum of the 3:1 elliptical jet in the center of the shear layer at $X/D_{MIN}=1.25$ is shown for the major axis plane in Fig. 7. A distinct peak at $f=2913$ Hz can be identified in the shear layer. This frequency, when scaled with θ_0, and the jet exit velocity U_0, yielded the Strouhal number $St=f\cdot\theta_0/U_0=0.019$. A similar velocity spectrum was obtained on the minor axis plane. A less conspicuous peak, at $f=2854$ Hz, could be detected on this plane. This peak frequency yielded a Strouhal number of 0.017. The values of the initial Strouhal numbers on both axis planes are close to

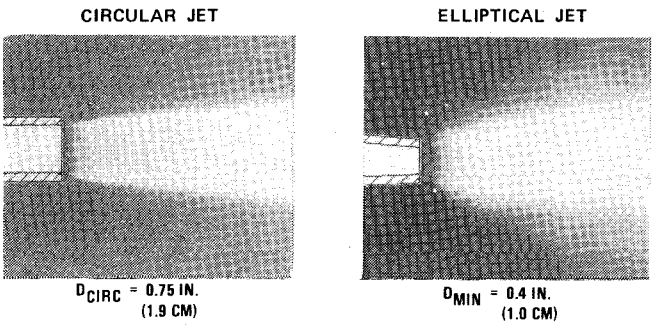

Fig. 8 Flame characteristics for circular and elliptical jets.

the most amplified frequency as predicted by linear instability theory. Therefore, $f \simeq 2900$ Hz was identified as the initial vortex shedding frequency f_i. Since f_i was nearly the same for the minor and major axes (2854 and 2913 Hz), the experiments showed that the elliptical nozzle shed one single uniform vortex in spite of the variation of θ_0. Morris and Miller[13] showed numerically that the shedding frequency of the elliptic jet did not change around the jet and was not dependent on its aspect ratio.

The frequency peaks in the elliptical jet shear layer indicate that coherent structures existed even in this highly turbulent flow. Similar observations were made in a high Reynolds number circular jet.[4] The peaks in the spectrum of the circular jet were less predominant than in the elliptical jet.

Combustion Tests

Fuel-rich plume combustion tests were performed to compare circular and elliptical nozzles. The plume exhaust velocity was subsonic.

Figure 8 shows a comparison of the flame boundary characteristics and spreading rates of the circular and 3:1 elliptical nozzles. It is obvious that the flame of the elliptical nozzle spread faster at the minor axis than the circular jet, even though D_{MIN} in this case was only about one-half of the circular jet diameter. The photographs also show a highly turbulent flame boundary for the elliptical jet compared to a smooth boundary for the circular jet.

The measurement of the combustor temperature distribution T_C confirmed that the elliptical jet spread at a higher rate than the circular jet, even in a high-velocity and high-temperature environment. A comparison between the three elliptical jets with aspect ratios of 2:1, 3:1, and 3.5:1 and the circular jet is given in Fig. 9. The most significant spread was observed in the elliptical jet with the 3:1 ratio. Both 2:1 and 3.5:1 jets have lower spreading rates in the minor axis plane than the third elliptical jet (3:1) and the circular jet. At $X/D_C = 0.4$ or $X/D_{CIRC} = 2.83$, the 3:1 jet spread on the minor axis side to the same T_C profile width as the circular jet, although the initial diameter of the minor axis was only about one-half of the circular jet diameter. In addition, significant spread occurred on the major axis side. The higher spreading rate of the 3:1 jet, relative to the other jets (2:1 and 3.5:1) was also measured in cold-flow tests.

The centerline temperature comparison between the 3:1 elliptical jet and the circular jet is shown in Fig. 10. This figure shows that the centerline temperature near the nozzle (except in the first diameter from the nozzle) was significantly higher in the elliptical jet than in the circular jet.

Discussion and Conclusion

Nonreacting and combustion tests were performed to compare mixing and combustion of fuel-rich plumes issued from circular and elliptical nozzles.

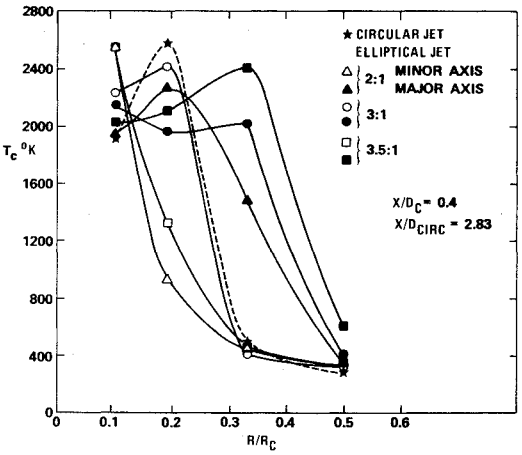

Fig. 9 Radial temperature distributions for circular and elliptical jets.

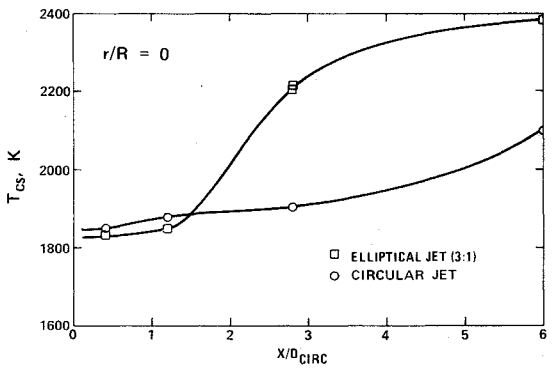

Fig. 10 Centerline temperature distributions for circular and elliptical jets.

The nonreacting tests showed that the elliptical jet spread faster than the circular jet, even at conditions of high Reynolds numbers, turbulent initial conditions, and coaxial airflow. The velocity spectra showed that the elliptical nozzles shed a single vortex around the nozzle lip in spite of the variation in θ_0 around the circumference of the nozzle lip. Yet, the distorted mean velocity contours near the elliptical nozzle exit indicated that high azimuthal modes of vortex motion were excited. It was also observed that the energy of the initial vortices was higher in the elliptical jet than in the circular jet. The same qualitative result, indicating more intense vortex activity in the elliptical nozzle, was obtained from the observed flame characteristics. In the tests with the elliptical nozzle, a highly turbulent flame boundary in the extreme fore end of the mixing region was observed compared to a nearly smooth flame boundary of the circular jet. It is suggested that the more intense vortex activity at the elliptical jet nozzle increased the fine-scale mixing in the fore end of the mixing region and enhanced combustion near the nozzle. This conjecture is supported by the higher experimental combustion temperatures near the elliptical nozzle compared to the circular nozzle. Therefore, it appears that when using elliptical nozzles, combustion can be achieved in regions near the nozzle exit where near-stoichiometric mixture ratios exist. This was not possible with circular nozzles under the same conditions. The higher temperatures may promote higher reaction rates. The comparison between the three elliptical nozzles with different eccentricity showed that the 3:1 ratio was most effective in enhancing mixing, in both cold- and hot-flow tests.

Acknowledgment

This work was partly supported by the U.S. Air Force Office of Scientific Research (AFOSR) and the Naval Sea Systems Command.

References

[1]Broadwell, J.E. and Breidenthal, R.E., "A Simple Model of Mixing and Chemical Reaction in a Turbulent Shear Layer," *Journal of Fluid Mechanics*, Vol. 125, 1982, pp. 397–410.

[2]Mungal, M.G. and Dimotakis, P.E., "Mixing and Combustion with Low Heat Release in a Turbulent Shear Layer," *Journal of Fluid Mechanics*, Vol. 148, 1984, pp. 349–382.

[3]Michalke, A., "On Spatially Growing Disturbances in an Inviscid Shear Layer," *Journal of Fluid Mechanics*, Vol. 23, No. 3, 1965, pp. 521–544.

[4]Schadow, K.C., Wilson K.J., Crump, J.E., Foster, J.B., and Gutmark, E., "Interaction Between Acoustics and Subsonic Ducted Flow with Dump," AIAA Paper 84-0530, 1984.

[5]Gutmark, E. and Ho, C.M., "The Development of an Elliptic Jet," *Bulletin of the American Physical Society*, Vol. 27, No. 9, 1982, p. 1184.

[6]Gutmark, E. and Ho, C.M., "Near Field Pressure Fluctuations of an Elliptic Jet," AIAA Paper 83-0663, 1983.

[7]Gutmark, E. and Ho, C.M., "On the Forced Elliptical Jet," *Proceedings of 4th Symposium on Turbulent Shear Flows*, Karlsruhe, FRG, 1983.

[8]Schadow, K.C., "Study of Gas-Phase Reactions in Particle-Laden, Ducted Flows," *AIAA Journal*, Vol. 11, July 1973, pp. 1042–1044.

[9]Abbott, S.W., Smoot, L.D., and Schadow, K.C., "Direct Mixing and Combustion Efficiency Measurements in Ducted, Particle-Laden Jets," *AIAA Journal*, Vol. 12, March 1974, pp. 275–282.

[10]Peters, N. and Williams, F.A., "Liftoff Characteristics of Turbulent Jet Diffusion Flames," *AIAA Journal*, Vol. 21, March 1983, pp. 423–429.

[11]Lee, M.J. and Schadow, K.C., "Detailed Flow Measurements in Fuel-Rich, Particle-Laden Plumes," *Proceedings of 20th JANNAF Combustion Meeting*, Monterey, CA, Oct. 1983.

[12]Schadow, K.C., "Fuel-Rich Particle-Laden Plume Combustion," *AIAA Journal*, Vol. 13, Dec. 1975, pp. 1553–1555.

[13]Morris, P.J. and Miller, D.G., "Wavelike Structures in Elliptic Jets," AIAA Paper 84-0399, 1984.